J Mater Sci: Mater Electron (2011) 22:929–935
DOI 10.1007/s10854-010-0239-z

# Characterization of Tin disulphide thin films prepared at different substrate temperature using spray pyrolysis technique

**K. Vijayakumar · C. Sanjeeviraja · M. Jayachandran · L. Amalraj**

Received: 22 July 2010 / Accepted: 19 October 2010 / Published online: 20 November 2010


**Abstract** Thin films of tin disulphide on glass substrates were prepared by spray pyrolysis technique using precursor solutions of $SnCl_2{\cdot}2H_2O$ and n–n dimethyl thiourea at different substrate temperatures varied in the range 348–423 K. Using the hot probe technique the type of conductivity is found to be n type. X ray diffraction analysis revealed the polycrystalline nature with increasing crystallinity with respect to substrate temperature. The preferential orientation growth of $SnS_2$ compound having hexagonal structure along (002) plane increased with the substrate temperature. The size of the tin disulphide crystallites with nano dimension were determined using the Full Width Half Maximum values of the Bragg peaks and found to increase with the substrate temperature. The surface morphology had been observed on the surface of these films using scanning electron microscope. The optical absorption and transmittance spectra have been recorded for these films in the wavelength range 400–800 nm. Thickness of these films was found using surface roughness profilometer. The absorption coefficient ($\alpha$) was determined for all the films. Direct band gap values were found to exist in all the films deposited at different substrate temperatures. The value of room temperature resistivity in dark decreased from $5.95 \times 10^3$ Ω cm for the amorphous film deposited at low temperature (348 K) to $2.22 \times 10^3$ Ω cm for the polycrystalline film deposited at high temperature (423 K) whereas the resistivity values in light decreased from $1.48 \times 10^3$ to $0.55 \times 10^3$ Ω cm respectively, which is determined using the four probe method. Activation energy of these thin films was determined by Arrhenius plot.

K. Vijayakumar
Department of Physics, K.L.N. College of Information Technology, Madurai 630 611, India

C. Sanjeeviraja
Department of Physics, Alagappa University, Karaikudi 630 003, India

M. Jayachandran
ECMS Division, Central Electrochemical Research Institute, Karaikudi 630 006, India

L. Amalraj (✉)
Department of Physics, V.H.N.S.N. College, Virudhunagar 626 001, India
e-mail: amalraj57@yahoo.co.in

## 1 Introduction

Metal chalcogenides thin films have been extensively studied due to their potential application in electronic, optical and superconducting devices [1, 2]. Tin chalcogenide belonging to IV–VI compound semiconductors has been attracting considerable interest in the field of photovoltaic energy conversion [3–7]. Among these semiconductors Tin disulphide ($SnS_2$) is a member of a class of compounds having the $CdI_2$ structure [8]. It has a layered structure and it can exist in a number of different polytypes [9, 10]. Synthesis of single crystal $SnS_2$ by chemical vapor transport method at low temperature using $SnCl_4$ as a transport agent [11].The results of the photo-conductivity effects [12–14], Raman spectra [15], electrical switching and conducting mechanism [16], high pressure measurement [17], XPS [18] and optical properties [8, 9, 19] of bulk $SnS_2$ have been reported by many workers. Only few papers have been reported in the formation of $SnS_2$ in thin film form [18, 20–27]. It has many important properties like n-type electrical conductivity [20, 21, 24, 25], high optical absorption coefficient ($>10^4$ $cm^{-1}$) in the visible

region [21], optical direct band gap values of 2.44–2.6 eV [21, 24, 25]. These properties suggest that the compound to be a promising material in the development of thin film solar cells [21]. Several binary sulphides of tin such as SnS (orthorhombic), $SnS_2$ (hexagonal), $Sn_2S_3$ (rhombic), and $Sn_3S_4$ (tetrahedral), among them SnS is a semiconducting material and exhibits both the n-type and p-type conduction depending on the concentration of tin [5]. The results of direct optical band gap and photoconductivity properties support the use of this material as a solar absorber in thin film solar cell and near-infrared detector [28, 29]. Ristov et al. [5] suggests that $SnS_2$ thin film can be used as a n-p heterojunction of n-$SnS_2$/p-SnS.

Thin films of $SnS_2$ were fabricated by various techniques like successive ionic layer adsorption and reaction [25], Atmospheric pressure chemical vapor deposition [26], chemical deposition [3, 7], vacuum evaporation [27, 30], chemical vapour transport [31], dip coating [23, 32], chemical spray pyrolysis [20, 21] and solvothermal process [33]. Each method has its own characteristics merits and demerits in producing homogeneous and defect free thin film nano materials and new preparation methods are being evolved to produce controlled size and shape of desired morphology [34]. Among them, spray pyrolysis method is principal to prepare tin disulphide thin film, which is low cost that can be used to deposit uniform coatings on large surface area [35]. Previous authors had reported the optical properties on nano $SnS_2$ thin films annealed in the temperature range 423–573 K [23] and the optical transmission measurements on $SnS_2$ single crystals were carried out in the lower temperature range 13–300 K [36] by other than spray pyrolysis method. In the present study, it is intended to prepare and characterize $SnS_2$ thin film on the glass substrate at the lower thermal energy range (348–423 K) by spray pyrolysis method using the precursor solutions of $SnCl_2{\cdot}2H_2O$ and thiourea.

## 2 Experimental details

A glass made double nozzle sprayer was designed and fabricated in our laboratory to prepare thin film samples by spray pyrolysis method. It is a coaxial assembly of two corning glass tubes, in which the diameters of inner and outer tubes are 6 and 14 mm, respectively. Both the tubes were tapered at one end with a tapering angle of 30° to form the spray nozzle. The glass substrates are well cleaned and kept inside the furnace. The furnace was resistively heated with kanthal wire and the temperature was controlled by a dimmer stat. A chromel–alumel thermocouple based temperature controller is used to monitor and measure the temperature of the substrates. The inner tube of the spray nozzle was connected to the air compressor and the outer tube to the solution reservoir. The carrier gas pressure was monitored by valve flow meter. The solution flow rate was determined with the help of a graduated burette as the reservoir.

The precursor solutions of $SnCl_2{\cdot}2H_2O$ and thiourea were dissolved separately in a solution containing de-ionised water and isopropyl alcohol in proper ratio. The molarities of tin and thiourea solutions were 0.04 and 0.08 M, respectively. A few drops of concentrated hydrochloric acid were added for complete dissolution. Equal volume of these two solutions were mixed together and sprayed on to the hot glass substrates with area of $75 \times 25$ mm$^2$. The precursor solutions were sprayed at different substrate temperature (348, 373, 398 and 423 K) and their films were prepared. The other deposition parameters like solution flow rate, carrier gas pressure and nozzle to substrate distance were kept as 3 ml/min, 0.7 kg/cm$^2$ and 24 cm respectively. After deposition of these films, it was allowed to cool to room temperature, cleaned with distilled water, dried and then stored in a dessicator. The colour of the deposited thin films is golden-yellow and adheres to the substrate.

The crystal structural study of these films were examined by the XPERT PRO diffractometer using Cu $K_\alpha$ radiation ($\lambda = 1.5406$ Å). The scanning angle $2\theta$ was varied in the range of 10°–80° in steps of 0.05°. The thickness of the sample was determined using Mitutoyo- SJ 301 surface roughness profilometer. The absorption coefficient ($\alpha$) of these thin films were determined in the wavelength range 400–800 nm using Shimadzu—UV 410S model double beam spectrophotometer by recording the absorption spectrum in the above wavelength range. The spectral data was used to determine the type of optical transition and the band gap present in the sample. The dark and photo-resistivities of the samples were measured using the four-probe technique with Keithly 2000 electrometer. The variation of electrical resistivity with temperature was studied from ambient temperature to 423 K. The variation of DC electrical resistivity with respect to temperature was analyzed using Arrhenius plot and the activation energy of the $SnS_2$ thin films were found out. The type of conductivity of these semiconductor thin films was determined using the hot probe technique.

## 3 Results and discussion

Figure 1a–d showed the XRD diffraction profiles of the Spray pyrolysised $SnS_2$ thin films with various substrate temperatures of 348, 373, 398 and 423 K, respectively. From Fig. 1a, the obtained film has no definite peaks, which may be attributed to lower thermal energy. At the substrate temperatures of 373 and 423 K, the mixed phases

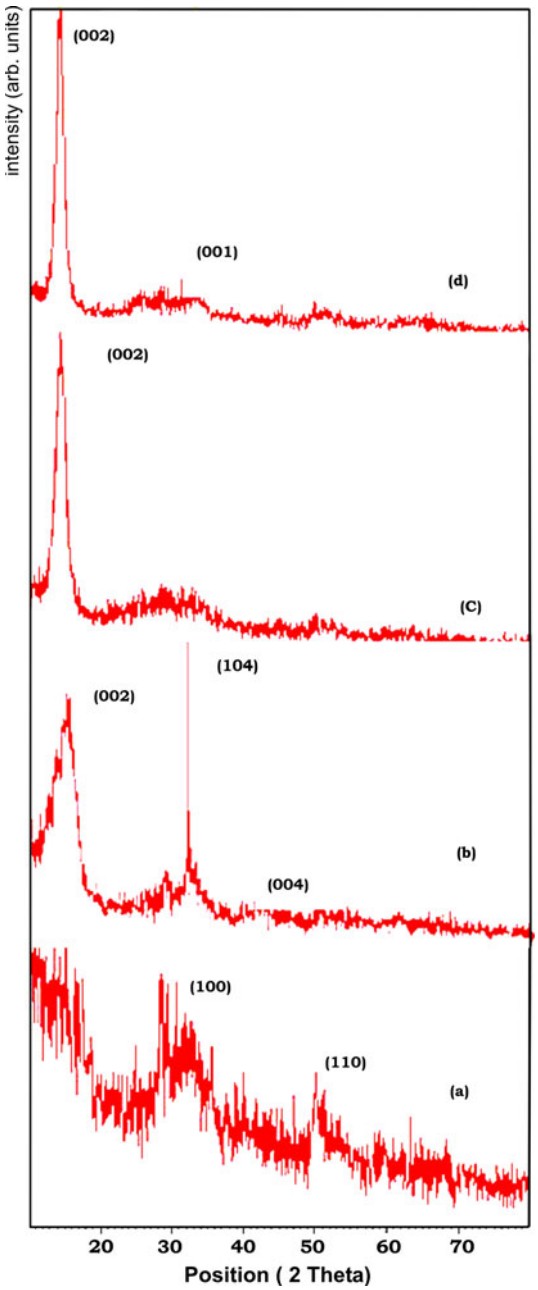


**Fig. 1** XRD pattern of $SnS_2$ thin film prepared at **a** 348 K **b** 373 K **c** 398 K and **d** 423 K

($SnS_2$, $Sn_2S_3$) are observed with broad Bragg peak value of $SnS_2$ is 14.94° (Fig. 1b) and 14.60° (Fig. 1d) respectively. Panda et al. [23] had been observed the broad peak value of 14.88° for $SnS_2$ thin film deposited by dip coating technique. At 398 K, the increase of crystallanity with the preferential orientation growth of $SnS_2$ compound having hexagonal structure along (002) plane (Fig. 1c) diffracted with single prominent Bragg peak at the $2\theta$ position 14.45°. The interplanar spacing corresponding to this peak is

**Table 1** The size of the crystallites of $SnS_2$ thin film with respect to temperature

| Substrate temperature (K) | Crystallite size (Å) |
|---|---|
| 373 | 35 |
| 398 | 53 |
| 423 | 71 |

determined to be 6.12 Å, which is higher than the standard value (5.90 Å) which cannot be attributed to any other phase of tin and sulphur. The value of lattice parameter c is determined to be 12.24 Å due to this hexagonal structure. It is found that the unit cell of this structure in the present study is elongated in c direction while comparing with the standard report of 11.80 Å [37]. The elongated strain may be attributed to lower thermal energy deposition of this compound with relatively lower concentration solutions of $SnCl_2$ precursor. Previous authors [24, 38] had observed strain in their $SnS_2$ thin films prepared by SILAR and plasma—enhanced chemical vapor deposition methods respectively.

From the Full Width at Half Maximum (FWHM) value of the peak obtained, the size of the tin disulphide crystallites was determined and tabulated in Table 1 using Debye–Scherrer formula [39].

The increase of substrate temperature, the crystallite size increased from 35 Å for the film grown at 373 K to 71 Å for the film grown at 423 K. This can be understood with the help of availability of thermal energy at different substrate temperatures. Amalraj et al. [20] also had reported the crystallite size of spray pyrolysised $SnS_2$ thin film is 63.9 Å at the substrate temperature of 513 K using the precursor solutions $SnCl_4$ and thiourea. Thangaraju and kaliannan [21] reported the size of the crystallite of spray pyrolysised $SnS_2$ thin film on the glass substrate and FTO coated glass substrate at the substrate temperature of 548 K is 115 and 324 Å respectively, using the same precursor solutions of present study. The reported crystallite size value is agreed closely [20] with the present data.

The surface morphology of the thin films deposited at different substrate temperatures were studied and analyzed by photographing the scanning electron microscope images of the above samples respectively as shown in Fig. 2. These SEM pictures were recorded with a same magnification of 5 k for comparison. It is seen from Fig. 2a, random shaped grains with an average size of 1.2 μm were formed at the substrate temperature of 348 K. As the substrate temperature increases to 423 K, the surface morphology of the films was found to become sandy structured nature with nanometer sized particles, which is clearly observed from Fig. 2d.

The observed grain size values from SEM images are much larger than the crystallite sizes measured from XRD

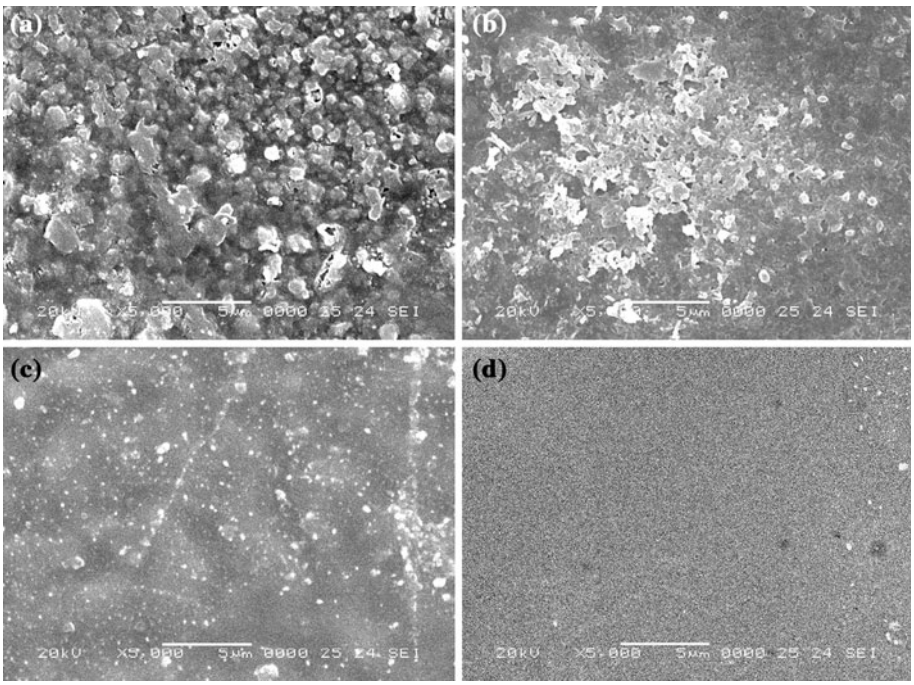


**Fig. 2** SEM image of the magnification 5 k of $SnS_2$ thin film at **a** 348 K **b** 373 K **c** 398 K and **d** 423 K

peaks. This is due to the fact that in SEM images, the grain size is measured by the distance between the visible grain boundaries. Each grain constitutes aggregates of several crystallites [40]. In XRD, the diffraction of X-ray takes place inside the tiny crystallites and hence the measured size is always in the nm range, which is very much less than the grain size measured from SEM image studies.

To study the optical properties of the materials, the optical absorption spectra of this spray pyrolysised $SnS_2$ thin film is recorded in the wavelength range 400–800 nm. Hence the optical transmittance (T) with respect to wavelength ($\lambda$) of spray pyrolysised $SnS_2$ thin film at different substrate temperature is calculated and plotted as shown in Fig. 3.

It was observed that there was a considerable increase in transmittance with increasing of substrate temperature, which may be due to increase in crystalline nature as the substrate temperature increases. This result is attributed by XRD analysis. From the absorbance spectrum the variation of the absorption coefficient $\alpha$ with respect to wavelength is calculated and plotted as shown in Fig. 4. It shows that the value of absorption coefficient $\alpha$ decreases exponentially as the wavelength increases from 400 to 800 nm.

In the high photon energy region, the energy dependence of the absorption coefficient $\alpha \geq 10^4$ $cm^{-1}$ suggests the occurrence of direct optical transition, which is investigated by the relation [41].

$$(\alpha h\nu)^n = k(h\nu - E_g) \quad (1)$$

Where k is the proportionality constant, $E_g$ is the optical band gap and n = 2 for a direct allowed transition. The

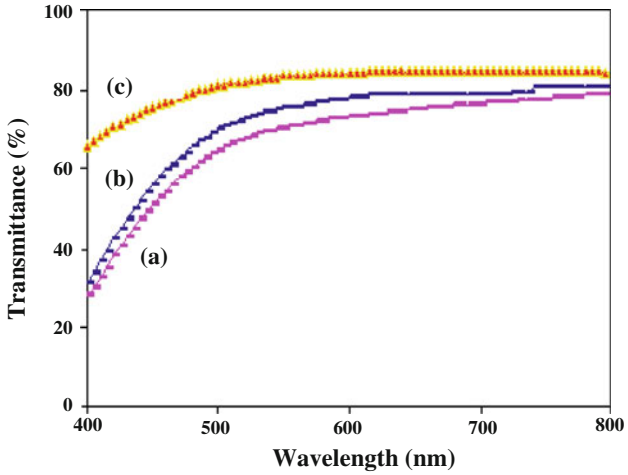


**Fig. 3** Transmittance spectra for $SnS_2$ thin film prepared at **a** 373 K **b** 398 K and **c** 423 K

band gap estimation of tin disulphide thin film achieved by plotting $(\alpha h\nu)^2$ as a function of $(h\nu)$ as shown in Fig. 5.

The plot yields a straight line which indicates a good fit, extrapolation of the straight line to $(\alpha h\nu)^2 = 0$ gives the optical direct band gap values for different substrate temperatures and is tabulated in Table 2.

The increase of substrate temperature, the direct allowed band gap values decreased from 2.80 to 2.65 eV. A similar behavior of decreasing of direct forbidden band gap values with increasing of temperature range 13–300 K was reported by Mandalidis et al. [36] on $SnS_2$ single crystals. Optical band gap measurements on $SnS_2$ single crystal [8, 9, 12, 17, 19] and thin film [3, 7, 21, 25, 30] have been

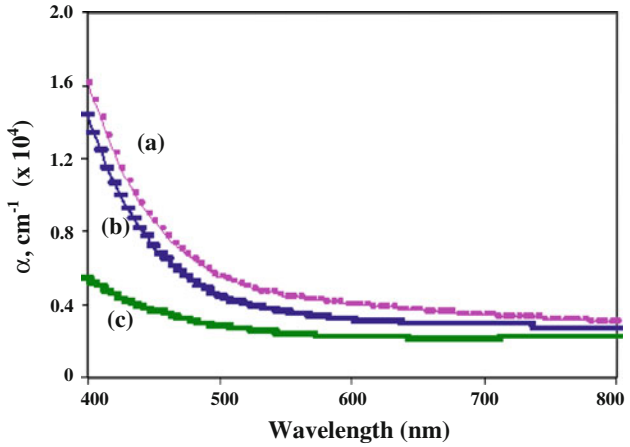


**Fig. 4** Absorption coefficient (α) spectra for $SnS_2$ thin film prepared at **a** 373 K **b** 398 K and **c** 423 K

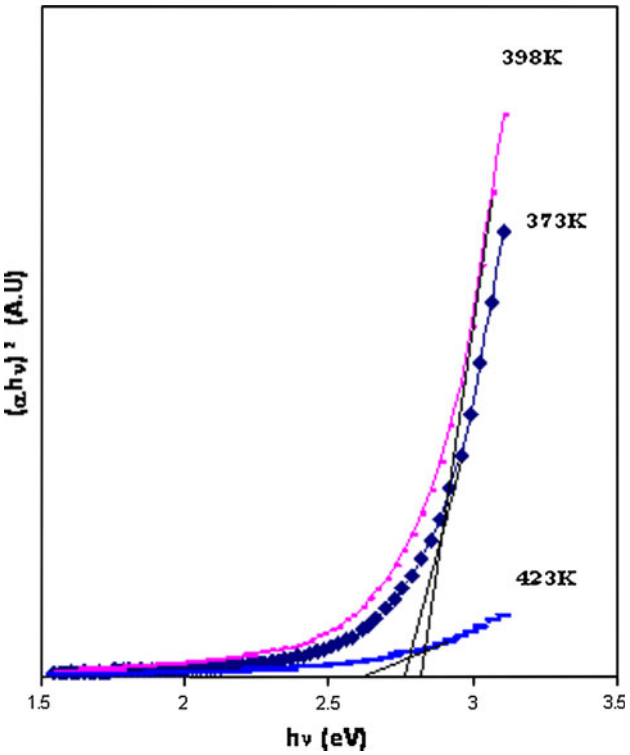


**Fig. 5** $(\alpha h\nu)^2$ vs $(h\nu)$ plot for $SnS_2$ thin film prepared at different substrate temperature

**Table 2** Band gap values of $SnS_2$ films with respect to substrate temperature

| Substrate temperature (K) | Band gap (eV) |
|---|---|
| 373 | 2.80 |
| 398 | 2.75 |
| 423 | 2.65 |

reported by previous workers. The direct allowed band gap values have been reported by [21] (2.44 eV) and [25] (2.6 eV). In the present study, even though the above such band gap in the ultraviolet region could not be observed due to glass substrate, a higher band gap of 2.80 eV at the substrate temperature 373 K with direct transition obtained here can be attributed to the nano crystallite formation of $SnS_2$, which is evident from XRD spectrum. The type of conductivity of $SnS_2$ thin film prepared in the present study show n- type electrical conductivity, which agrees well with the reported literatures [20, 21, 24, 25]. The DC room temperature electrical resistivity of $SnS_2$ thin film is determined using four probe technique at the different substrate temperature and their values are tabulated in Table 3.

**Table 3** Electrical resistivity values of $SnS_2$ films with respect to different substrate temperature

| Substrate temperature (K) | Electrical resistivity in dark ($\times 10^3$ Ω cm) | Electrical resistivity in light ($\times 10^3$ Ω cm) |
|---|---|---|
| 348 | 5.95 | 1.48 |
| 373 | 4.45 | 1.12 |
| 398 | 3.28 | 0.81 |
| 423 | 2.22 | 0.55 |

This shows the photo conducting nature of the n-type $SnS_2$ thin film, which could be used as a light sensitive material. The variation of resistivity of the as prepared film with respect to temperature was determined. A decrease in the resistivity is found as the temperature of the sample is increased which predicts the n-type semiconductor nature of the $SnS_2$ thin film deposited in the present study. Sankapal et al. [25] had observed the dark resistivity of $SnS_2$ thin film is in the order of $10^3$ Ω-cm. The reported value is the same range as the present value, but agreed closely [21] with the present data.

The activation energy of $SnS_2$ thin film can be calculated by the formula

$$\rho = \rho_o \exp(-E_a/KT) \quad (2)$$

where $\rho_o$ is a pre-exponential factor and $E_a$ is the activation energy. Both of which are determined by the best fit of the experimental data to Eq. (2). The Arrhenius plot is drawn with this experimental data as shown in Fig. 6, which it can be predicted that the variation of resistivity of this $SnS_2$ film is being assisted by a single activation process with an activation energy is tabulated in Table 4, which are determined by the best fit of the experimental data to Eq. (2). The Arrhineus plot is drawn as shown in Fig. 6a–d for various substrate temperatures.

Sankapal [25] also had reported the activation energy of $SnS_2$ film is 0.37 eV at ambient temperature. Amalraj et al. [20] had reported a similar single step activation process with activation energy of 0.25 eV at the substrate temperature 458 K for the $SnS_2$ thin film prepared by the same method using $SnCl_4{\cdot}5H_2O$ as one of the precursors.

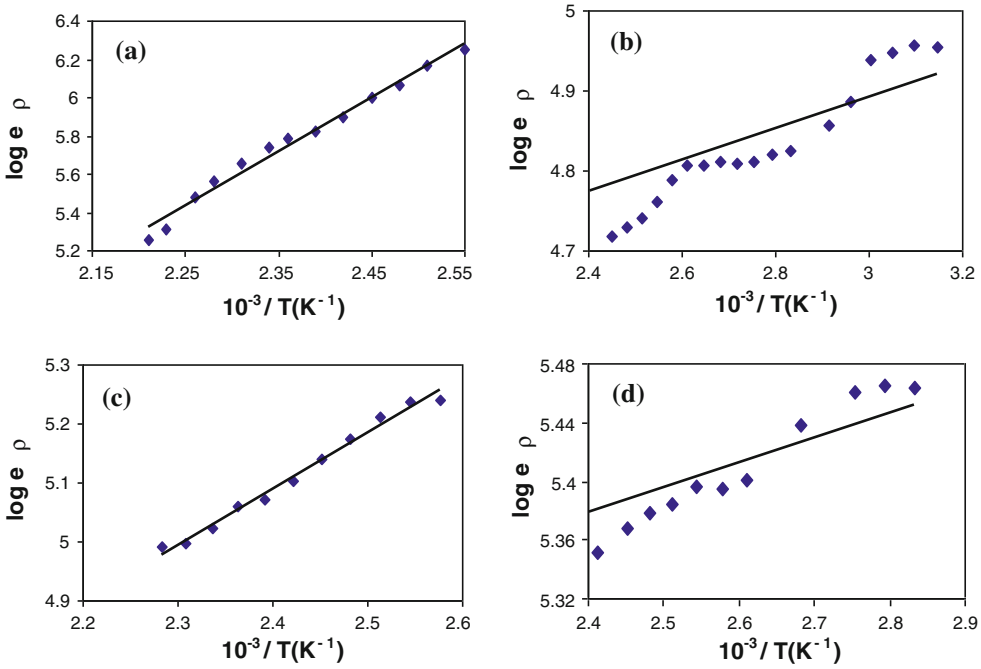


**Fig. 6** Variation of electrical resistivity for $SnS_2$ thin film prepared at substrate temperature **a** 348 K **b** 373 K **c** 398 K and **d** 423 K

**Table 4** Activation energy of $SnS_2$ film with respect to different substrate temperature

| Substrate temperature (K) | Activation energy (eV) |
|---|---|
| 348 | 1.12 |
| 373 | 0.12 |
| 398 | 0.47 |
| 423 | 0.12 |

Kawano et al. [27] had observed a two- step process of activation for their vacuum deposited amorphous $SnS_2$ thin film. They found activation energy of 0.26 eV below 242 K and 0.47 eV above 242 K with pre-exponential values of $0.041 \times 10^2$ and $4.34 \times 10^{-2}$ Ω cm respectively. Lokhande [7] also had observed a two-step activation process with activation energies of 0.43 and 1.52 eV in two different temperature regions for his amorphous $SnS_2$ films. Such differences in activation energies may be due to varying preparation parameters and the presence of different defect states during the growth of $SnS_2$ thin films.

## 4 Conclusions

Golden yellow coloured thin films of $SnS_2$ crystallite with nano dimensions had been deposited on to glass substrate by spray pyrolysis using the precursor solutions of $SnCl_2{\cdot}2H_2O$ and n–n dimethyl- thiourea at relatively lower substrate temperatures. Polycrystalline nature of the film with hexagonal structure grown with high preferential orientation of (002) miller plane at 398 K with strain is identified. The film is found to exhibit n-type electrical conduction. The spray pyrolysised thin film shows direct allowed optical transition nature with a higher band gap values. A thermal activation process with an activation energy values are determined with respect to the substrate temperature and the room temperature resistivity values are determined in dark and light respectively and found to have photo conducting nature, which suggest that this $SnS_2$ thin film could be a potential candidate for opto- electronic as well as thin film solar cell devices.

## References

1. R. Suryanarayanan, Physica Status Solidi B **85**, 9 (1978)
2. K. Rajeshwar, Appl. Electrochem. **15**, 1 (1985)
3. R.D. Engelken, H.E. Mc Cloud, C. Lee, M. Slayton, J. Electrochem. Soc. **134**, 2696 (1987)
4. H. Noguchi, A. Setiyadi, H. Tanamura, T. Nagamoto, O. Omoto, Sol. Energy Mater. Sol. Cells **35**, 325 (1994)
5. M. Ristov, G. Sinadinovski, I. Grozdanor, Thin Solid Films **173**, 53 (1989)
6. M.T.S. Nair, P.K. Nair, Semicond. Sci. Technol. **6**, 132 (1991)
7. C.D. Lokhande, J. Phys. D Appl. Phys. **23**, 1703 (1990)
8. D.L. Greenway, R. Nitsche, J. Phys. Chem. Solids **26**, 1445 (1965)
9. P.A. Lee, G. Said, R. Davis, T.H. Lim, J. Phys. Chem. Solids **30**, 2719 (1969)
10. S. Acharya, O.N. Srinivasa, Physica Status Solidi A **56**, K1 (1979)
11. T. Shibata, T. Miura, T. Kishi, T. Nagai, J. Cryst. Growth **106**, 593 (1990)
12. G. Domingo, R.S. Itoga, C.R. Kannewurf, Phys. Rev. **143**, 536 (1996)
13. S.G. Patil, R.H. Tredgold, J. Phys. D Appl. Phys. **4**, 718 (1971)

14. R. Nakata, M. Yamaguchi, S. Zembutsu, M. Sumita, J. Phys. Soc. Japan **32**, 1153 (1972)
15. D.G. Mead, J.C. Irwin, Solid State Commn. **20**, 885 (1976)
16. G. Said, P.A. Lee, Physica Status Solidi A **15**, 99 (1973)
17. M.J. Powell, J. Phys. C Solid State Phys. **10**, 2967 (1977)
18. J.H. Shephard, P.M. Williams, J. Phys. C Solid State Phys. **7**, 4416 (1974)
19. M.Y. Au-Yang, M.L. Cohen, Phys. Rev. **178**, 1279 (1969)
20. L. Amalraj, C. Sanjeeviraja, M. Jayachandran, Cryst. Growth **234**, 683 (2002)
21. B. Thangaraju, P. Kaliannan, J. Phys. D Appl. Phys. **33**, 1054 (2000)
22. J. George, K.S. Joseph, J. Phys. D Appl. Phys. **15**, 1109 (1982)
23. S.K. Panda, A. Antonakos, Mat. Res. Bull. **42**, 576 (2007)
24. N.G. Deshpande, A.A. Sagade, Y.G. Gudage, C.D. Lokhande, J. Alloy Compd. **436**, 421 (2007)
25. B.R. Sankapal, R.S. Mane, C.D. Lokhande, Mater. Res. Bull. **35**, 2027 (2000)
26. L.S. Price, I.P. Parkin, A.M.E. Hardy, R.J.H. Clark, Chem. Mater. **11**, 1792 (1999)
27. K. Kawano, R. Nakata, M. Sumita, J. Phys. D Appl. Phys. **22**, 136 (1989)
28. P. Pramanik, P.K. Basu, S. Biswas, Thin Solid Films **150**, 269 (1987)
29. N.K. Reddy, K.T.R. Reddy, Thin Solid Films **325**, 4 (1998)
30. J. George, K.S. Joseph, J. Phys. D Appl. Phys. **15**, 1109 (1982)
31. K. Matsumoto, K. Tagaki, J. Cryst. Growth **63**, 202 (1983)
32. S.C. Roy, M.K. Karanjai, Thin Solid Films **350**, 72 (1999)
33. B. Hai, K. Tang, C. Wang, J. Cryst. Growth **225**, 92 (2001)
34. B.G. Jeyaprakash, R. Ashok kumar, K. Kesavan, A. Amalarani, J. Am. Sci. **6**, 22 (2010)
35. B. Thangaraju, P. Kaliannan, Cryst. Res. Technol. **35**, 71 (2000)
36. S. Mandalidis, J.A. Kalomiros, K. Kambas, J. Mat. Sci. **31**, 5975 (1996)
37. X ray Powder Diffraction JCPDS file reference no. 21—1231
38. A. Ortiz, A. Sanchez-juarez, J. Elec. Chem. Soc. **147**, 3708 (2000)
39. P.H. Klug, L.E. Alexander, *X-Ray Diff. Procedures* (Wiley, New York, 1954)
40. R.N. Panda, M.F. Hsieh, R.J. Chung, T.S. Chin, J. Phys. Chem. Solids **64**, 193–199 (2003)
41. J. Bardeen, F.J. Blatt, L.H. Hall, in *Proceedings of the Photoconductivity Conference*, Atlantic city (Wiley, New York, 1956) p. 146